TECHNICAL ARTICLE

X-ray diffraction characterization of magnetostriction in Terfenol-D

Mark A. Rodriguez [ORCID],a) Mina Faltas, Nichole R. Valdez, and Daniel R. Lowry

Sandia National Laboratories, P.O. Box 5800, Albuquerque, NM 87185, USA

The magnetostrictive response of a Terfenol-D pellet was measured via a laboratory-based X-ray diffractometer. X-ray diffraction patterns were collected from the pellet sample with and without the presence of an applied magnetic field ($\sim$30 mT) generated by placing a large magnet under the pellet. A standard reference material, Silicon 640c, was employed as an internal standard. Magnetostriction values of 323 and 227 ppm $\Delta l/l$ were determined for the (104) and (110) indexed peaks, respectively, assuming a rhombohedral structure for Terfenol-D. A threshold noise level value of $\sim$20 to 30 ppm $\Delta l/l$ was suggested based on before/after measurements in the absence of the applied field. No clear evidence of domain wall rotation was detected via changes in relative intensities of diffraction peaks in the presence of the applied magnetic field.

I. INTRODUCTION

Magnetostriction is a change in the dimension of a material when experiencing an applied magnetic field. These changes are often small, on the order of 10^{-6} m/m, and can be difficult to observe without special measurement methods. Strain gauges are often used for measuring magnetostriction of bulk samples but are not sensitive enough for thin-film type geometries. Other techniques such as light dilatometry and light interferometry have found use for measuring magnetostriction. The dilatometry method uses a Fiber Bragg Grating and can be a much more sensitive measurement of magnetostriction. Lanza et al. (2011) demonstrated the use of this method for detecting magnetostriction of Terfenol-D ($Tb_{0.3}Dy_{0.7}Fe_2$). Likewise, Xu and Chen (2014) employed a light interferometer to measure deflection of a cantilever where the magnetostrictive material was deposited on the cantilever device. These above-mentioned methods are considered "bulk" and do not yield crystallographic material responses. The desire to measure the magnetostrictive response via crystallographic changes to the material led to the use of X-ray diffraction (XRD) as a means of monitoring magnetostriction. There are limited reports of this type of work in the literature. This is primarily because the material's response is very weak and requires extremely careful analysis to detect and quantify a magnetostrictive response (Arakawa et al., 2005). Hence, XRD has not served as a routine method for the detection of magnetostriction. With the advent of materials with a high magnetostrictive response, XRD is beginning to be employed as a diagnostic tool for magnetostriction.

Recently, Nie et al. (2016) performed in-situ XRD analysis of $Tb_{0.4}Dy_{0.6}Fe_2$ via synchrotron radiation. This compound, similar to the composition for the compound named Terfenol-D ($Tb_{0.3}Dy_{0.7}Fe_2$), was monitored with varying magnetic fields while simultaneously collecting XRD data. Their configurations allowed for variations in the magnetic field of up to $\sim$0.7 T, where a powder sample of a similar strong magnetostrictive material was analyzed within a capillary holder. In their work, Nie et al. (2016) did not document the diffraction peak shift in 2θ angle due to the applied magnetic field but instead showed relative intensity changes for diffraction peaks as the field was increased. This change in peak intensity observed by Nie et al. (2016) was attributed to domain wall motion under significant magnetic fields. Nie et al. (2016) did not report on the Terfenol-D composition $Tb_{0.3}Dy_{0.7}Fe_2$ in their study.

Having observed that XRD methods can be employed to monitor the magnetostrictive response, it was proposed that the use of a laboratory-based XRD system could potentially be employed for measuring magnetostriction on materials that displayed a strong material response. The exemplar material proposed for characterization would preferably be a commercially available material with a very large magnetostrictive response (>1000 ppm $\Delta l/l$). Terfenol-D (composition $Tb_{0.3}Dy_{0.7}Fe_2$) was chosen as an exemplar to investigate the possible presence of small changes in the crystal structure related to the magnetostriction response via XRD characterization.

II. EXPERIMENTAL PROCEDURE

Figure 1 shows the instrumental setup for the XRD experiment. The XRD system employed was a Bruker D8 Discover diffractometer equipped with a sealed tube X-ray source

---

a)Author to whom correspondence should be addressed. Electronic mail: marodri@sandia.gov
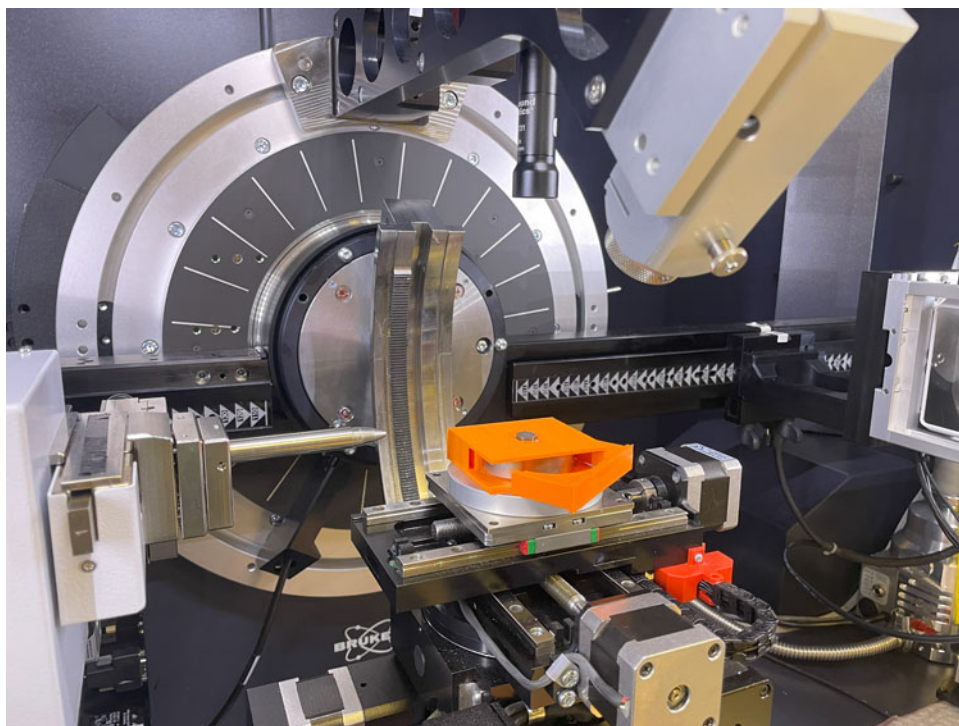
Figure 1. Experimental configuration for the in-situ XRD measurement of a mounted Terfenol-D pellet utilizing a specially designed 3D-printed holder.

(Cu Kα radiation), an incident beam mirror optic, 1-mm pinhole collimator, XYZ translation stage, laser/video alignment system, and a Dectris Eiger2 R 500 K CMOS area detector. The instrument goniometer radius was 336 mm. The Terfenol-D sample employed for this measurement was a pellet of dimension 1-cm diameter × 2-mm thick. NIST Silicon 640c standard powder was employed for correction of the measured XRD peak locations. A special 3D-printed holder was designed for our measurements and fabricated from acrylonitrile butadiene styrene (ABS) plastic. The holder design provided a stable and reliable reference height for the sample during analysis. This holder would allow for the loading and unloading of a high-field magnet directly under the pellet as shown in Figure 1. The pellet sample was loaded on top of a 3D-printed holder and a small piece of double-sided carbon tape was employed between the pellet and the top portion of the holder to keep the sample from moving during the XRD analysis.

To assure the highest accuracy for peak locations, a very thin layer of Silicon 640c powder was dusted onto the surface of the pellet. This method allowed simultaneous measurement of the Terfenol-D and Si peaks with and without the applied field. The Si peaks served as a means of peak location correction, as these peak positions are based on the NIST-reported lattice parameter for Silicon 640c which is certified to 0.00001 Å (Cline et al., 2000). This enabled the measurement of interplanar spacings (d values) for the Terfenol-D with the high accuracy needed to monitor the very small changes generated by the applied field. To obtain the best possible XRD pattern data, XRD scans were collected from 24° to 120° 2θ, with a step size of 0.01° and a very slow scan rate. Total data collection time per scan was 14 h. The sample was initially analyzed without the magnet to establish the baseline peak positions for the Terfenol-D. Next, the ∼30-mT magnet (K&J Magnetics, Inc.) was placed under the pellet and the scan was repeated to detect changes in the peak location

indicative of a magnetostrictive response. Finally, the magnet was removed and a final XRD scan was performed to see whether the material would display similar structural responses to that of the initial state. Prior to each scan, the sample was aligned via the laser-alignment system as the sample can move slightly when the magnet is placed under the pellet and when removed for subsequent zero field measurements. Great care was taken during placement and removal of the magnet as the strong fields from the magnet would be drawn towards the iron-bearing parts of the instrument. Additionally, careful attention was paid to the use of the double-sided tape to assure that the pellet would not move during loading and unloading of the magnet as the Terfenol-D pellet would often desire to rotate upwards to stand on-end if it was not properly secured in place. A check of the alignment laser position at the conclusion of the experiment verified that the pellet did not physically move during the data collection process. These details were critical to obtain quality XRD data for subsequent analyses.

III. RESULTS AND DISCUSSION

Figure 2 shows the results for the XRD measurement. The right side of the figure shows a stack XRD with the initial, applied field, and final XRD patterns. On first appearance, the results look identical. However, the expected changes would likely be very subtle and so require careful evaluation of the data. The Powder Diffraction File (PDF) entries (Kabekkodu et al., 2024) are plotted below the patterns to show the expected peak locations. A pattern for $TbFe_2$ (PDF entry 04-007-2009) was employed as a surrogate phase for the similar Terfenol-D phase $Tb_{0.3}Dy_{0.7}Fe_2$ to identify the peak locations for the magnetostrictive phase. It was noted that the relative intensity of the Terfenol-D peak profile at ∼54.6° 2θ was considerably higher than the intensities reported for $TbFe_2$ as shown in the stick pattern below the
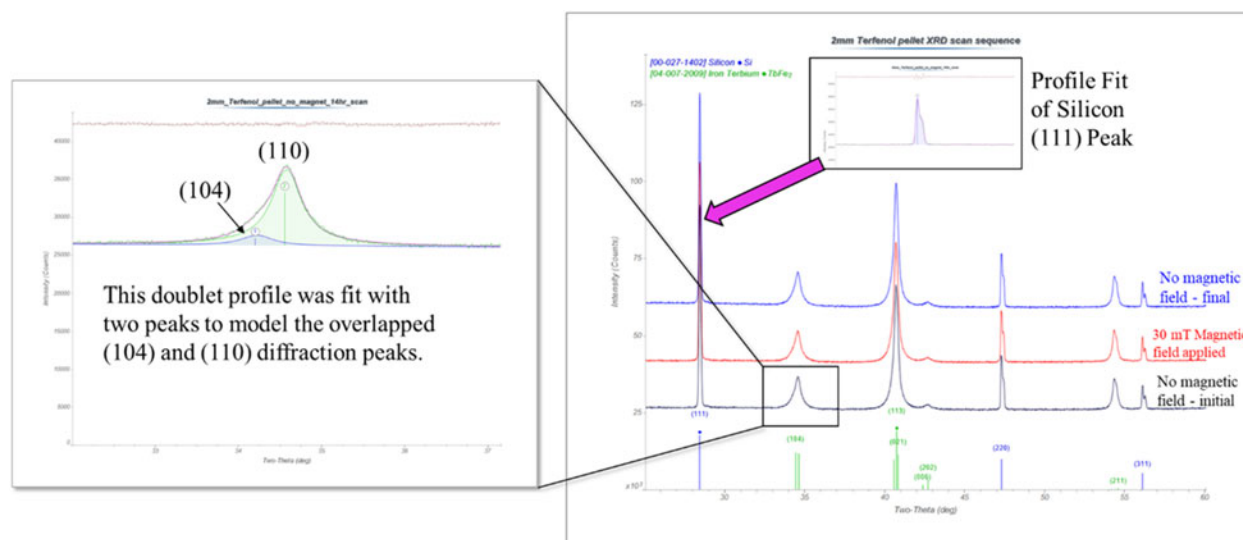
Figure 2. Right: The *initial*, *applied field*, and *final* XRD patterns collected on the Terfenol-D pellet (inset shows zoomed view of a Si peak from Si 640c standard). Left: Zoomed view of Terfenol-D peaks showing fitting of two overlapped peaks from the Terfenol-D phase.

XRD scans in Figure 2. This could suggest some preferred orientation effects for the Terfenol-D phase when compared to the surrogate $TbFe_2$ phase. An inset is shown for the XRD stack plot on the right of Figure 2, which shows a Si (111) peak from the Si 640c standard. This inset illustrates the profile fit result that was employed to determine the 2θ peak location. Profile fitting was performed using JadePro (ver 9.0) software (Materials Data, Inc.). On the left side of Figure 2, data are presented for the Terfenol-D peaks between 32° and 37° 2θ. Unfortunately, there is no documented PDF entry for Terfenol-D with the similar rhombohedral structure to that of $TbFe_2$. In fact, the exact structure of Terfenol-D ($Tb_{0.3}Dy_{0.7}Fe_2$) is not fully understood, being in close proximity to a morphotropic phase boundary (Bergstrom et al., 2013). However, the appearance of the tail on the low-angle side of diffraction profile for the Terfenol-D XRD patterns indicates a break from cubic symmetry and is self-consistent with the material having the rhombohedral unit cell similar to that reported for $TbFe_2$. Hence, for the purposes of this analysis, we assume the Terfenol-D to display the rhombohedral symmetry with a structure similar to that of $TbFe_2$ where we index the peaks employing the hexagonal setting of the unit cell similar to those reported for the PDF entry of $TbFe_2$. Previously, Chelvane et al. (2009) reported a cubic form of $TbFe_{1.95}$ (PDF entry 04-017-6675), which, in appearance, looks very similar to the XRD pattern for the rhombohedral structure. The difference between the cubic and rhombohedral structure is the very subtle separation of the diffraction peaks as the structure breaks from the cubic to the lower symmetry rhombohedral structure. Because of the nature of the rhombohedral symmetry and defined unit cell, most of the observed profiles from the Terfenol-D peaks in the XRD patterns were convolutions of two or more (*hkl*) planes. This was unfortunate and made determination of exact peak location difficult because the XRD pattern required the fitting of as many as three or four peaks under a single observed profile. The most straightforward profile for the Terfenol-D phase with relatively good diffraction intensity was that of the (104) and (110) doublet, because the unit cell predicted only two reflections present within this profile. Therefore, this

profile was easier to model, requiring fewer constraints, and generated less uncertainty regarding the refined peak locations obtained from the fit. With this assessment, two peaks were fit for the profile shown in Figure 2 (left), where constraints were employed to model the profile. These peaks, with Miller indices of (104) and (110) for the rhombohedral unit cell (hexagonal setting), were modeled using a Pearson VII function where peak widths and shape functions were constrained to be equivalent for the two overlapped peaks. In addition, the profile-fitting model accounted for the $K\alpha_1/K\alpha_2$ doublet intensity profile that was present in all the XRD patterns. This model for profile-fitting was utilized for analysis of the relevant Terfenol-D peak 2θ segments of each XRD pattern as well as the 2θ segments of the Si reflections, and the refined peak locations were corrected based on the known Si peak locations for each pattern. From these peak locations, straightforward determination of interplanar spacing (*d*) values were obtained via the corrected 2θ peak locations as documented in Table I. This table shows the observed 2θ peak locations, corrected 2θ values based on the Si internal standard, and *d* values derived from corrected 2θ positions. To determine the error in the peak location, the peak profiles were fit multiple times to determine the reproducibility of the obtained 2θ value based on the modeling algorithm. Because the peaks were modeled with the above outlined constraints, the reproducibility of the peak 2θ angle location was excellent. The (110) peak changed only ±0.0001° 2θ which translates to an error in *d*-spacing of ±0.00001 Å for this peak. The (104) peak demonstrated a higher error in reproducibility due to its lower intensity, yielding a variability of ±0.0004° 2θ, which translates to an error in *d*-spacing of ±0.00007 Å. The Si peaks are also reported in Table I to demonstrate that the applied peak location corrections were employed properly. The 2θ correction for the Terfenol-D (104) and (110) peaks was based on a linear interpolation of the $\Delta 2\theta$ offsets for the Si peaks at their respective angles as shown in Table I. An attempt to model the correction function was made where the additional (311) Si peak was included and a parabolic 2θ correction employed. This model was not significantly different from the linear model based on the Si (111) and (220)

TABLE I.   Refined peak positions for Si 640c and Terfenol-D with and without the applied magnetic field

Series	Phase	(hkl)	NIST 2θ (°)	2θ observed (°)	2θ error (°)	2θ corrected (°)	d corrected (Å)
Initial – no field	Silicon	(111)	28.4409	28.4339	−0.0070	28.4409	3.13570
Initial – no field	TbFe₂	(104)		34.1937	−0.0065	34.2002	2.61968
Initial – no field	TbFe₂	(110)		34.5506	−0.0064	34.5570	2.59345
Initial – no field	Silicon	(200)	47.3003	47.2948	−0.0055	47.3003	1.92022
Applied magnetic field	Silicon	(111)	28.4409	28.4309	−0.0100	28.4409	3.13570
Applied magnetic field	TbFe₂	(104)		34.1792	−0.0096	34.1888	2.62053
Applied magnetic field	TbFe₂	(110)		34.5394	−0.0095	34.5489	2.59404
Applied magnetic field	Silicon	(200)	47.3003	47.2917	−0.0086	47.3003	1.92022
Final – magnetic field removed	Silicon	(111)	28.4409	28.4333	−0.0076	28.4409	3.13570
Final – magnetic field removed	TbFe₂	(104)		34.1947	−0.0064	34.2011	2.61961
Final – magnetic field removed	TbFe₂	(110)		34.5517	−0.0063	34.5580	2.59337
Final – magnetic field removed	Silicon	(200)	47.3003	47.2966	−0.0037	47.3003	1.92022

peaks. Due to its lower overall intensity and little value-added improvement to the angular correction, the Si (311) peak was excluded in favor of the more straightforward linear correction model for 2θ.

Based on the resulting interplanar spacing (d), the change in the interplanar spacing can be derived as a function of the magnetic field. Table II documents the corrected d values for the initial (no field), applied magnetic field state, and final state once the magnet was removed. One would expect that the applied field would show a change in the length from that of the initial state, and once the field was removed the sample would return to a state similar to the initial condition. Table II documents this effect, showing an increase in the interplanar spacing with the applied field for both the (104) and (110) peaks and subsequent contraction of the d value to a value similar to the initial state after magnet removal. While the changes are small (i.e., between 0.00059 and 0.00085 Å), the results do confirm that detection of the magnetostrictive response is possible through changes in the interplanar spacing of the material via XRD analysis.

Figure 3 shows a graphical form of the magnetostriction response for the two monitored Terfenol-D peaks. This figure shows that when the magnetic field is applied, both reflections show an expansion of >200 ppm, consistent with a magnetostrictive response. Subsequent removal of the magnetic field revealed a loss of this expansion. In fact, the final $\Delta l/l$ value did not return to the initial value, but resulted in a contracted value (approximately ∼25 to 30 ppm contraction) compared to the initial condition. This might be a result of a slightly expanded initial state of the pellet due to inadvertent exposure to the magnet prior to the measurement or could indicate an approximate level of error associated with the measurement. If the latter is true, a value of ∼20 to 30 ppm might serve as an estimate of sensitivity for this technique (i.e., noise level). The magnetostrictive response measured under the applied field is approximately an order of magnitude larger than this possible noise level and supports confirmation of

the detected materials response. These results are encouraging as a proof-of-principle demonstration for detecting a magnetostrictive response in a laboratory setting and specifically demonstrates this field-induced response via data linked to a crystallographic change of the structure. This is an important differentiating factor for the XRD method as compared to the other methods of measurement. The difference in $\Delta l/l$ values between the (104) and (110) indices might also suggest an anisotropic response of the rhombohedral structure where the unit cell may more readily expand in the c-axis direction as indicated by the 323-ppm response of the (104) planes which have a component of c-axis dependence as compared to the lower value of 227 ppm for the (110) planes which have no c-axis dependence.

In contrast to the work of Nie et al. (2016), our analysis did not observe significant changes in XRD peak intensity related to the application of the applied field. As mentioned earlier, Nie et al. (2016) documented the relative changes in peak intensities with varying applied magnetic fields from 0.02 to 0.69 T. For their experiment, the strength of the highest magnetic field was several orders of magnitude higher than that of the magnet used in our study. Nie et al. (2016) attributed the intensity changes observed in their XRD patterns to domain rotation, resulting in reorientation of crystalline domains and hence changes in scattering intensity at the detector for a given set of (hkl) planes. In this study, the lack of significant changes in diffracted intensity with our changes in applied field suggests that for our magnetic field strength and our samples, the domain wall rotation has not yet been achieved within the lower field strength of the employed magnet (∼30 mT) and the overall geometry of the experimental setup. In addition, the pellet nature of our sample may have greater geometrical constraints than that of the powder sample employed by Nie et al. (2016). Therefore, it may be our Terfenol-D composition and geometry is merely demonstrating the initial magnetostrictive response of the material prior to significant domain wall rotation, which typically occurs at

TABLE II.   Changes in the interplanar spacing (d value) before, during, and after applied magnetic field and derivation of the corresponding magnetostrictive response $\Delta l/l$ (ppm)

Terfenol-D (hkl)	$d_{initial}$ (Å)[a]	$d_{applied}$ (Å)[a]	$d_{applied}-d_{initial}$ (Å)	$\Delta l/l$ (ppm)	d_{final} (Å)[a]	$d_{final}-d_{initial}$ (Å)	$\Delta l/l$ (ppm)
(104)	2.61968	2.62053	0.00085	**323**	2.61961	−0.00007	−26
(110)	2.59345	2.59404	0.00059	**227**	2.59337	−0.00008	−28

[a]Typical errors for derived d-spacings were ±0.00001 Å for the (110) peak and ±0.00007 Å for the (104) peak based on profile-fitting.
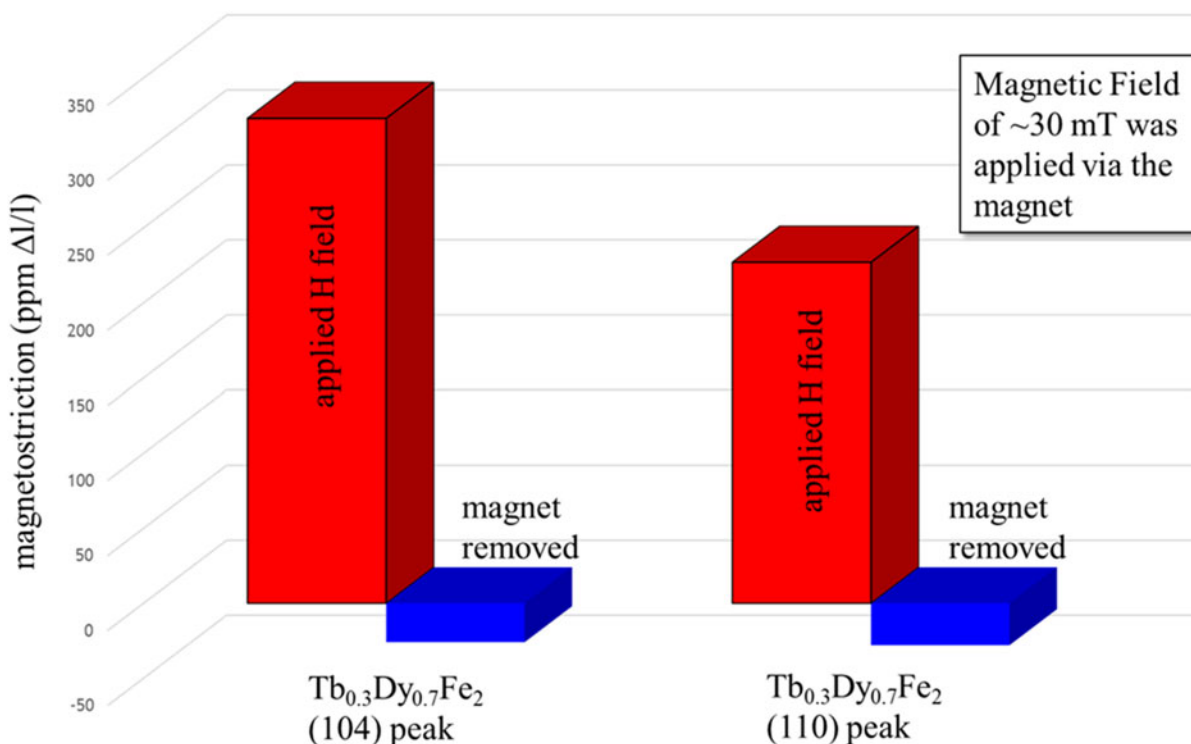
Figure 3. Magnetostrictive responses of Terfenol-D based on $\Delta l/l$ of (104) and (110) d value measurements. Results indicate that the detection of magnetostriction can be performed via the employed XRD protocol.

higher magnetic field strengths. The lower field strength used in this experiment (~30 mT) may only be activating the well-aligned grains parallel to the field direction to respond with a magnetostrictive behavior. More energy from a higher field may be needed to overcome the resistance to domain wall movement and allow for the observation of relative intensity changes as more domains orient to the higher field.

IV. CONCLUSION

The magnetostrictive response has been successfully observed via the use of laboratory-based XRD instrumentation. Critical attention to the precise measurement protocol is required to correct XRD peak positions via a calibration standard. Additionally, employment of meticulous profile-fitting methods to determine peak locations is also required for a successful outcome. With this employed methodology, a material response of >200 ppm was observed for Terfenol-D under an applied field of 30 mT. A possible sensitivity level of ~20 to 30 ppm was estimated based on initial and final conditions of zero applied field. Additionally, a possible anisotropic dependence of the magnetostrictive response was detected based on comparison of the measured (104) and (110) reflections where the (104) plane showed a more significant magnetostrictive response relative to the (110) plane. The ability to probe magnetostriction properties via laboratory-based XRD instrumentation enables a crystallographic diagnostic for materials research of these important materials.

COMPETING INTERESTS

The authors declare none.

REFERENCES

Arakawa, E., K.-i. Maruyama, K. Mori, H. Nishigaitsu, and N. Aizawa. 2005. "Magnetostriction Observed by X-Ray Diffraction in Iron." *IEEE Transactions on Magnetics* 41 (10): 3718–20. doi:10.1109/TMAG.2005.854922.

Bergstrom, R., Jr., M. Wuttig, J. Cullen, P. Zavalij, R. Briber, C. Dennis, V. O. Garlea, and M. Laver. 2013. "Morphotropic Phase Boundaries in Ferromagnets: $Tb_{1-x}Dy_xFe_2$ Alloys." *Physical Review Letters* 111: 017203. doi:10.1103/PhysRevLett.111.017203

Chelvane, J. A., M. Palit, H. Basumatary, S. Pandian, and V. Chandrasekaran. 2009. "Structural, Magnetic and Mössbauer Studies on Magnetostrictive $Ho_{1-x}Tb_xFe_{1.95}$ [x = 0-1]." *Physica B: Condensed Matter* 404 (8-11): 1432–1436. doi:10.1016/j.physb.2008.12.043.

Cline, J. P., R. D. Deslattes, J. L. Staudenmann, E. G. Kessler, L. T. Hudson, A. Henins, and R. W. Cheary. 2000. "NIST Certificate, SRM 640c Line Position and Line Profile Standard for Powder Diffraction." National Institute of Standards and Technology, Gaithersburg, MD 20899. Accessed December 12, 2024. https://tsapps.nist.gov/srmext/certificates/archives/640c.pdf

Kabekkodu, S., A. Dosen, and T. Blanton. 2024. "PDF-5+: A Comprehensive Powder Diffraction File™ for Materials Characterization." *Powder Diffraction* 39 (2): 47–59. doi:10.1017/S0885715624000150.

Lanza, G., G. Breglio, M. Giordano, A. Gaddi, S. Buontempo, and A. Cusano. 2011. "Effect of the Anisotropic Magnetostriction on Terfenol-D Based

Fiber Bragg Grating Magnetic Sensors." *Sensors and Actuators A: Physical* 172 (2): 420–427. doi:10.1016/j.sna.2011.10.005.

Nie, Z., S. Yang, Y.-d. Wang, Z. Wang, D. Liu, Y. Ren, T. Chang, and R. Zhang. 2016. "In-Situ Studies of Low-Field Large Magnetostriction in $Tb_{1-x}Dy_xFe_2$ Compounds by Synchrotron-Based High-Energy X-Ray Diffraction." *Journal of Alloys and Compounds* 658: 372–6. doi:10.1016/j.jallcom.2015.10.244.

Xu, Y.-g., and X.-g. Chen. 2014. "On Relationship Between Annealing Treatment and Magnetostriction Behavior of Fe-16Cr-2.5Mo Damping Alloy." *Journal of Alloys and Compounds* 582: 364–368. doi:10.1016/j.jallcom.2013.08.070.